ORIGINAL RESEARCH ARTICLE

Journal of Cellular Physiology WILEY

Matrix stiffness controls cardiac fibroblast activation through regulating YAP via AT$_1$R

Lele Niu[1,2] | Yuanbo Jia[1,2] | Mian Wu[1,2] | Han Liu[1,2] | Yanjing Feng[3] | Yan Hu[1,2] | Xiaohui Zhang[1,2] | Dengfeng Gao[3] | Feng Xu[1,2] | Guoyou Huang[1,2,4] ⓘD

[1]The Key Laboratory of Biomedical Information Engineering of Ministry of Education, Xi'an Jiaotong University, Xi'an, China

[2]Bioinspired Engineering and Biomechanics Center (BEBC), Xi'an Jiaotong University, Xi'an, China

[3]Department of Cardiology, The Second Affiliated Hospital of Xi'an Jiaotong University, Xi'an, China

[4]Department of Engineering Mechanics, School of Civil Engineering, Wuhan University, Wuhan, China

Correspondence
Guoyou Huang, The Key Laboratory of Biomedical Information Engineering of Ministry of Education, Xi'an Jiaotong University, 710049 Xi'an, China.
Email: wwgyhuang@xjtu.edu.cn

Abstract

Cardiac fibrosis is a common pathway leading to heart failure and involves continued activation of cardiac fibroblasts (CFs) into myofibroblasts during myocardium damage, causing excessive deposition of the extracellular matrix (ECM) and thus increases matrix stiffness. Increasing evidence has shown that stiffened matrix plays an important role in promoting CF activation and cardiac fibrosis, and several signaling factors mediating CF mechanotransduction have been identified. However, the key molecules that perceive matrix stiffness to regulate CF activation remain to be further explored. Here, we detected significantly increased expression and nuclear localization of Yes-associated protein (YAP) in native fibrotic cardiac tissues. By using mechanically regulated in vitro cell culture models, we found that a stiff matrix-induced high expression and nuclear localization of YAP in CFs, accompanied by enhanced cell activation. We also demonstrated that YAP knockdown decreased fibrogenic response of CFs and that YAP overexpression promoted CF activation, indicating that YAP plays an important role in mediating matrix stiffness-induced CF activation. Further mechanistic studies revealed that the YAP pathway is an important signaling branch downstream of angiotensin II type 1 receptor in CF mechanotransduction. The findings help elucidate the mechanism of fibrotic mechanotransduction and may contribute to the development of new approaches for treating fibrotic diseases.

KEYWORDS
cardiac fibrosis, hydrogel, mechanical microenvironment, mechanotransduction, Yes-associated protein

1 | INTRODUCTION

Cardiac fibroblasts (CFs), a major cell type in the heart, play an important role in maintaining the normal function of the heart (Kong et al., 2019; Park et al., 2018). In response to abnormal changes in biochemical cues (e.g., angiotensin II, interleukin-6, transforming growth factor-β1 [TGF-β1]) in various cardiovascular diseases, CFs can be activated into myofibroblasts to initiate a 'reparative' fibrosis. Although the architecture of repaired tissue is remodeled, it eventually forms scar tissue and continuously secretes extracellular matrix (ECM; mainly type I and III collagen), leading to arrhythmia and the development of heart failure (Hale, 2016; Morine et al., 2018; Yokoe et al., 2003). The stiffness of fibrotic myocardium can dramatically increase (up to two to three times of normal range) due to the excessive deposition and excess crosslinking of the ECM during fibrosis (Frankenreiter et al., 2017; Galie, Westfall, & Stegemann, 2011; Lee et al., 2017; Yong et al., 2016).

Moreover, the stiffened matrix was recently shown to function independently or cooperatively to promote the activation of CFs, thus forming a positive feedback loop to accelerate fibrosis (Herum, Choppe, Kumar, Engler, & Mcculloch, 2017; Mouton et al., 2019; Yong et al., 2015; Zhao et al., 2014). Accordingly, approaches targeting matrix stiffness and CF mechanobiology may hold promise in the prevention and the treatment of cardiac fibrosis (Flevaris et al., 2017; Bourhis et al., 2013; Vadon-Le Goff et al., 2011). Therefore, elucidation of the underlying mechanisms of mechanotransduction in CFs in response to a stiffened matrix is important.

Various signaling factors have been reported in CF mechanotransduction (Herum, Lunde, McCulloch, & Christensen, 2017), including danger-associated molecular patterns as stress-induced initiators of fibrosis (Bryant et al., 2015), syndecan-4 as a mechanosensory apparatus affecting collagen expression (Couchman, 2010), and myocardin-related transcription factors liberated from G-actin that enter the nucleus and promote fibrosis (Mouillerson, Langer, Guettler, Mcdonald, & Treisman, 2011). However, the key molecules that perceive matrix stiffness to regulate CF activation remain remain to be fully identified. Recently, Hippo pathway transcriptional coactivators, for example, Yes-associated protein (YAP) and transcriptional coactivator with PDZ-binding motif (TAZ), have been found to function as universal mechanotransducers (Dupont et al., 2011; Panciera, Azzolin, Cordenonsi, & Piccolo, 2017). Importantly, YAP has been shown to play important roles in various types of fibrosis. For instance, in liver fibrosis, YAP activation was found to be a critical driver of hepatic stellate cell activation and the inhibition of YAP represents a novel approach for the treatment of liver fibrosis (Mannaerts et al., 2015). In kidney diseases, YAP overexpression in cultured podocytes was shown to increase the abundance of ECM-related proteins that promote fibrosis (Rinschen, Grahammer, Huber, Benzing, & Schermer, 2017). In cancer, increased matrix stiffness has been found to enhance YAP activation in cancer-associated fibroblasts (CAFs), establishing a feedforward, self-reinforcing network that helps to maintain the CAF phenotype (Calvo et al., 2013). Despite these important findings, the role of YAP in CF mechanotransduction and cardiac fibrosis remains elusive.

Mechanistically, matrix stiffness may regulate YAP activity through different upstream signaling pathways (Nakajima et al., 2017; Schroeder & Halder, 2012; Wang et al., 2016). For instance, the mechanosensory proteins (vinculin and talins, as well the focal adhesion kinase (FAK) and Src-family of kinases) have been discovered in YAP and TAZ mechanotransduction (Hu et al., 2017; Panciera et al., 2017; Taniguchi et al., 2015). Interestingly, recent studies found that mechanosensitive YAP/TAZ signaling promotes the survival of stiffness-primed human dermal fibroblasts by controlling the expression of antiapoptotic protein BCL-XL, prompting efforts to therapeutically target YAP/TAZ and myofibroblast apoptosis (Hinz & Lagares, 2020; Lagares et al., 2017). In addition, it has been also demonstrated that YAP/TAZ-mediated mechanosignaling drives lung fibroblast activation in part through TGF-β-independent plasminogen activator inhibitor-1 (YAP/TAZ transcriptional target;

Liu et al., 2015). Recently, G-protein-coupled receptors (GPCRs) in the cell membrane have been found to mediate biochemical cues to either activate or inhibit the Hippo-YAP pathway (Yu et al., 2012; Low et al., 2014). Specifically, activation of $G\alpha12/13$-coupled receptor by lysophosphatidic acid (LPA) or sphingosine 1-phosphate (S1P) could enhance YAP activity by inhibiting Lats1/2 kinases (Yu et al., 2012). In contrast, the activation of Gs-coupled receptors by epinephrine or glucagon stimulation could inhibit YAP activity by increasing Lats1/2 kinase activity (Yu et al., 2012). Although several types of GPCRs have also been found to allow cells to sense mechanical cues (Makino & Schmid-Schönbein, 2006; Scholz, Monk, Kittel, & Langenhan, 2016), the relationship between these GPCRs and YAP in cell mechanotransduction is still unclear. Our recent work demonstrated that the blocking of angiotensin II type 1 receptor (AT_1R, the first GPCR identified as a mechanosensor [Schnitzler, Storch, & Gudermann, 2011]) with losartan significantly inhibited the activation of CFs to myofibroblasts induced by a stiff substrate (Yong et al., 2016). Given these findings, we speculate that YAP may function as an important downstream signaling molecule of AT_1R in mediating matrix stiffness-induced CF activation.

In this study, we first characterized the expression of YAP in native fibrotic tissues obtained from rat models of myocardial infarction (MI). We then investigated the role of YAP in matrix stiffness-induced CF activation by culturing CFs on mechanically tunable gelatin hydrogels. Finally, we explored the relationship between YAP and AT_1R in CF mechanotransduction. Our results identified an important role of YAP in mediating matrix stiffness-induced CF activation and established the YAP pathway as an important signaling branch downstream of AT_1R in CF mechanotransduction, thus promoting the understanding and treatment of fibrosis from a mechanobiological point of view.

2 | MATERIALS AND METHODS

2.1 | Animal experiments

Male Sprague-Dawley (SD) rats were provided by the Experimental Animal Center of Xi'an Jiaotong University School of Medicine. All male rats were housed in cages under hygienic conditions with a 12-hr light/dark cycle at 23 ± 3°C and 40–60% humidity for 7 days before the experiments. The male rats were provided with a commercial standard rat cube diet and freely available drinking water.

An MI model was developed by ligation of the proximal left coronary artery. In brief, animals were anesthetized by intraperitoneal injection (35 mg/kg). The heart was exposed, and the left coronary artery was ligated 2-3 mm from its origin between the left atrium and pulmonary artery conus by using a 6-0 polypropylene. Then, the thoracotomy was closed in multiple layers. A successful MI model was confirmed by regional cyanosis and ST-segment elevation in an electrocardiogram. The heart was obtained after 4 weeks of staining and Western blot analysis. All animal procedures followed

2.2 | Preparation and characterization of gelatin hydrogels

For preparation of gelatin hydrogels, a 4% wt/vol concentrated enzyme solution containing microbial transglutaminase (mTG; Ajinomoto, Japan) and deionized water was prepared. A 20% wt/vol solution of gelatin (Type A, Bloom 175; MP Biomedicals) was also prepared by adding gelatin and warm deionized water and mixing at 50°C until the protein was dissolved. These solutions were stored in a refrigerator at 4°C. Following preparation, the concentrated mTG solution was removed and heated at 37°C for 5 min, and the frozen gelatin solution was melted at 50°C before use. Different concentrations of mTG-gelatin solution were added to a six-well plate and incubated at 37°C for 3 hr to fully crosslink the gelatin. Finally, phosphate buffer saline (PBS) was added into the plate to allow swelling equilibrium of the hydrogels for 24 hr.

Atomic force microscopy (AFM; (Picoplus 5400; Agilent) was used to determine the stiffness of the gelatin hydrogels by indentation. Gelatin hydrogels on 35 mm dishes were swollen to equilibrium in PBS and indented at a velocity of 10 μm/s. Young's modulus was computed using the Hertz model (Roduit et al., 2008):

$$f = \frac{2}{\pi} \times \frac{E}{1 - v^2} \times \tan\alpha \times \delta,$$

where f is the indentation force, E is the Young's modulus to be determined, v is the Poisson ratio of the materials (here, we set its value as 0.5), α is the half opening angle of the tip (here is 35°), and δ is the indentation depth.

For characterization of the water-absorption capacity of the gelatin hydrogels, the wet weights of the hydrogels after swelling equilibrium were measured, and the dry weights of the hydrogels were obtained after freeze-drying using a vacuum freeze dryer (Songyuan Huaxing, China). For characterization of the degradation of the hydrogels, hydrogels on 35 mm dishes were soaked in PBS with 1× trypsin–EDTA (0.25% vol/vol; Thermo Fisher Scientific) at 37°C and the wet weights were sequentially measured after 10, 30, and 60 min.

2.3 | Cell isolation and culture

CFs were isolated from the hearts of neonatal SD rats (1–3 days old). We noted that CFs may show differences in phenotypes based upon their in vivo source. Nevertheless, both neonatal and adult CFs consistently undergo phenotype switching to myofibroblasts when cultured on rigid substrates in vitro, sharing similar expression profiles to cardiac myofibroblasts in vivo under pathological condition (Santiago et al., 2010). Therefore, CFs from the hearts of both neonatal and adult animals have been extensively used in research. We used neonatal CFs because they can be easily isolated and purified from neonatal hearts, which are more likely to be pathogen- and disease-free than adult hearts. In brief, heart tissues were excised following euthanasia by cervical dislocation and digested using collagenase type II enzyme (MP Biomedicals). Then the pellets were obtained by centrifuging the digested heart tissues. The pellets were resuspended in cell culture medium containing Dulbecco's modified Eagle's medium: nutrient mixture F-12 (DMEM/F-12; HyClone), 10% fetal bovine serum (FBS; Gibco), and 1% penicillin/streptomycin (Gibco). After the samples were plated for 45 min at 37°C and 5% CO_2, the supernatant of cell culture medium, including cardiomyocytes, was removed, and the remaining adherent cells were CFs. The CFs were directly seeded on gelatin hydrogels and cultured for 7 days on the matrices before analysis.

2.4 | Cell transfection and inhibition

YAP knockdown was performed in CFs by using a small interfering RNA (siRNA). The control cells were transfected with a control siRNA (5′-UUCUCCGAACGUGUCACGUTT). The siRNA transfections were performed with Lipofectamine™ 2000 (Life Technologies) in Opti-MEM I reduced serum medium (Invitrogen) according to the manufacturer's instructions. The target sequence of siRNA was 5′-GGUCAGAGAUACUUCUUAATT for rat YAP.

YAP overexpression was performed in the CFs by using a plasmid. The CFs were seeded into six-well plates coated with gelatin hydrogels. Then, a preincubated mixture containing 50 μl of Opti-MEM, 1.6 μg of DNA, and 1 μl of Lipofectamine 2000 was added into each well. After 6 hr, the medium was replaced, and the cells were allowed to recover for 72 hr before analysis.

For inhibition of AT_1R, the cells were treated with 10 μM losartan potassium (LP; Selleckchem), or the corresponding amount of DMSO diluted in complete media on Day 3. The treatment lasted for 4 days, and the culture medium with LP was changed in the middle of the experiment; therefore, the cells were redosed once.

2.5 | Immunohistochemistry

For tissue staining, heart tissues from the normal control (NC) and MI rats were preserved as paraffin-embedded samples. The paraffin-embedded sections were blocked in 10% goat serum (Thermo Fisher Scientific) and subsequently incubated with primary rabbit anti-rat YAP (1:400; Cell Signaling Technology; 14074), and anti-α-smooth muscle actin (anti-α-SMA) antibody (1:1,000; Boster, China; BM0002) in Tris-buffered saline–Tween 20 (TBST) that contained 5% bovine serum albumin (BSA; MP Biomedicals). Goat anti-rabbit IgG-horseradish peroxidase (HRP) (1:100; Dako, China; P0448) was used as a secondary antibody. Cell nuclei were visualized with 4',6-diamidino-2-phenylindole (DAPI) (1 μg/ml; Sigma; D9542). 3,3′-Diaminobenzidine tertrahydrochloride (DAB) Horseradish Peroxidase Color Development Kit (Hat Biotechnology, China; IS015) was used for chromogenic

development. Microphotographs were acquired and analyzed with an inverted fluorescence microscope (Olympus IX81, Japan) and ImageJ 6.0 (National Institutes of Health).

2.6 | Immunofluorescence staining and image analysis

Cells were fixed in 4% paraformaldehyde for 10 min followed by cell membrane permeabilization with 0.5% triton X-100. Then, the samples were blocked for 45 min at room temperature in blocking solution (5% BSA in PBS). The following antibodies were used: α-SMA-FITC antibody (1:500; Sigma; F3777), Ki-67 antibody (1:400; Cell Signaling Technology; 9129), and YAP antibody (1:100; Cell Signaling Technology; 14074). Alexa Fluor 488 goat anti-rabbit antibody (1:1,000; Thermo Fisher Scientific; A11034) was used as the secondary antibody, and the sections were further incubated at 37°C for 1.5 hr. Rhodamine phalloidin (1:1,000; Thermo Fisher Scientific; R415) was used to stain actin cytoskeleton. Cell nuclei were visualized with DAPI (1 μg/ml; Sigma; D9542).

For calculation of the total YAP and the ratio of nuclear YAP to cytoplasmic YAP (nuc/cyto YAP), immunofluorescent staining for DAPI/F-actin/YAP was used. The cell spreading area and nuclear boundaries were divided by thresholding of each color channel. The total YAP and the ratio of nuc/cyto YAP were then calculated using the formula:

$$\text{Total YAP} = \frac{\sum' \text{nuc}}{A_{\text{nuc}}} + \frac{\sum' \text{cyo}}{A_{\text{cyo}}},$$

$$\text{Ratio of nuc/cyto YAP} = \frac{\sum' \text{nuc}/A_{\text{nuc}}}{\sum' \text{cyo}/A_{\text{cyo}}},$$

where $\sum'$nuc represents the sum of the intensity values for the pixels in the nuclear region, $\sum'$cyo is the sum of intensity values for the pixels in the nonnuclear cytoskeleton area, A_{nuc} is the nuclear area, and A_{cyo} is the nonnuclear cytoskeleton area.

2.7 | Western blot analysis

First, the acquired tissues were ground by liquid nitrogen and the lysate was added. Then, the system was moved to ice for 20 min after being homogenized by five strokes. The supernatant was obtained by centrifuging the desired protein solution. The cells were directly cleaved by lysate with radioimmunoprecipitation assay at 4°C for 30 min. Finally, the supernatant was harvested by centrifugation at 4°C and 12,000 rpm for 10 min. Then, the protein lysates were processed following standard procedures. Ten micrograms of each protein sample was separated on 10% sodium dodecyl sulfate-polyacrylamide gels and transferred onto polyvinylidene difluoride membranes (Millipore). The membranes were blocked with TBST and 5% BSA and then incubated with primary antibodies at 4°C overnight. The following antibodies were used: glyceraldehyde-3-phosphate dehydrogenase (GAPDH) antibody

(1:1,000; Cell Signaling Technology; 2118), α-SMA antibody (1:1,000; Cell Signaling Technology; 19245), pYAP antibody (1:1,000; Cell Signaling Technology; 13008), and YAP antibody (1:1,000; Cell Signaling Technology; 14074). Then, the membranes were washed three times with TBST and incubated with goat anti-rabbit HRP-conjugated antibody (1:5,000; Cell Signaling Technology; 7074) for 2 hr at room temperature. A chemiluminescence system (ChemiScope 3300 Mini, China) was used to detect the bands after three washes with TBST. The exposed protein bands were quantified with ImageJ program.

2.8 | Real-time polymerase chain reaction (RT-PCR)

The total RNAs of the CFs on gelatin hydrogels were harvested by using an RNA extraction kit Tiangen, China). An UV-Vis spectrophotometer (NanoDrop2000; Thermo Fisher Scientific Inc.) was used to measure the concentration of total RNAs. A high capacity RevertAid First Strand cDNA Synthesis Kit (Thermo Fisher Scientific; K1622) was used to transcribe the extracted RNA into cDNA by polymerase chain reaction (PCR). Quantitative real-time PCR (qRT-PCR) was conducted by using SYBR® Premix Ex Taq™ II (Takara, China; RR820A) on a 7500 Fast Real-Time PCR System (Applied Biosystem). The relative mRNA expression was quantified by using the $2^{-\Delta\Delta C_t}$ method and internally normalized to GAPDH. The primer sequences are as follows: *GAPDH*: fwd CTTCTCTTGTGACAAAGTGGACAT, rev CTTGCCGTGGGT AGAGTCAT; *YAP*: fwd TACATAAACCATAAGAACAAGACCACA, rev GCTTCACTGGAGCACTCTGA; *α-SMA*: fwd CGATAGAACA CGGCATCATC, rev CATCAGGCAGTTCGTAGCTC; *Col I*: fwd GGTGAGACAGGCGAACAAGGTG, rev GCCAGGAGAGCCAGG AGGAC; *TGF-β1*: fwd CTTCAATACGTCAGACATTCGG, rev CA CAGTTGACTTGAATCTCTGC; transcription factor 21 (*TCF21*): fwd ACTGGCTCCCTCAGCGATGTAG, rev ACCCTCCTCGGTG CTCTCATTG; adipocyte platelet-derived growth factor receptor-α (*PDGFR-α*): fwd CAGGCAGGGCTTCAACGGAAC, rev AGTCTG GCGTGTGTCCATCTCC; cysteine-rich 61 (*CYR61*): fwd ATCTCC ACACGAGTTACCAATGACAAC, rev CCACAAGGACGCACTTC ACAGATC; connective tissue growth factor (*CTGF*): fwd CTCTT CTGCGACTTCGGCTC, rev GTACACGGACCCACCGAAGA.

2.9 | Statistical analysis

Statistical analysis was conducted by using GraphPad Prism 6 (GraphPad Software). Statistics are presented as the mean ± standard deviation for all quantitative data, with $n = 5$ for the mechanical tests and animal experiments, and $n \geq 3$ for the cell experiments. Two-tailed Student's *t*-test was performed for comparisons between two groups of samples. Multiple comparisons among the three or four experimental groups with a single varying parameter were performed using one-way analysis of variance with Tukey's post hoc testing (*$p < .05$, **$p < .01$, ***$p < .001$, and ****$p < .0001$).

3 | RESULTS

3.1 | YAP and AT$_1$R highly expressed in rat MI models

To verify whether YAP is involved in the pathology of MI, we performed double immunohistochemical and immunofluorescence staining for YAP and α-SMA in the MI and NC cardiac tissues. Immunohistochemical analysis revealed that both YAP and α-SMA were significantly increased in the MI tissue compared with the NC tissue (Figure 1a). Moreover, we found increased nuclear staining of YAP in the MI tissue compared with the NC tissue (Figure 1a). Immunofluorescence staining of the heart section also showed much higher expression of α-SMA and YAP in the MI tissue than in the NC tissue (Figures 1b and S1). From quantitative analysis, we found that the α-SMA$^+$ cells with nuclear YAP increased in the MI tissue compared with that of the NC tissue (Figure S1b). These results indicated that YAP may be involved in MI-induced cardiac fibrosis. We also tested the expression of AT$_1$R in vivo. The protein levels of AT$_1$R and pERK1/2 were significantly increased in the MI tissue compared with

the NC tissue, as confirmed by Western blot analysis (Figure 1c). These results confirmed that AT$_1$R is activated in MI-induced cardiac fibrosis.

3.2 | The expression and nuclear localization of YAP increased in CFs cultured on a stiff matrix

Mechanically, a notable characteristic during fibrosis is matrix stiffening, which has been shown to promote CF activation, thus accelerating the development of fibrosis via a positive feedback mechanism (Engler et al., 2008). To determine whether YAP is a regulator that senses microenvironmental stiffness and mediates the mechanical cue into a fibrosis-promoting signal in CFs, we fabricated gelatin hydrogels with different stiffnesses (4-41 kPa) to mimic those of the NC and MI heart tissues (Figure S2a). By varying the concentration of mTG used to crosslink the gelatin (10% gelatin as the final concentration) from 0.5% mTG to 2% mTG, we altered the stiffness of the gelatin hydrogels from 4 to 41 kPa. The results of water absorption and degradation experiments did not show
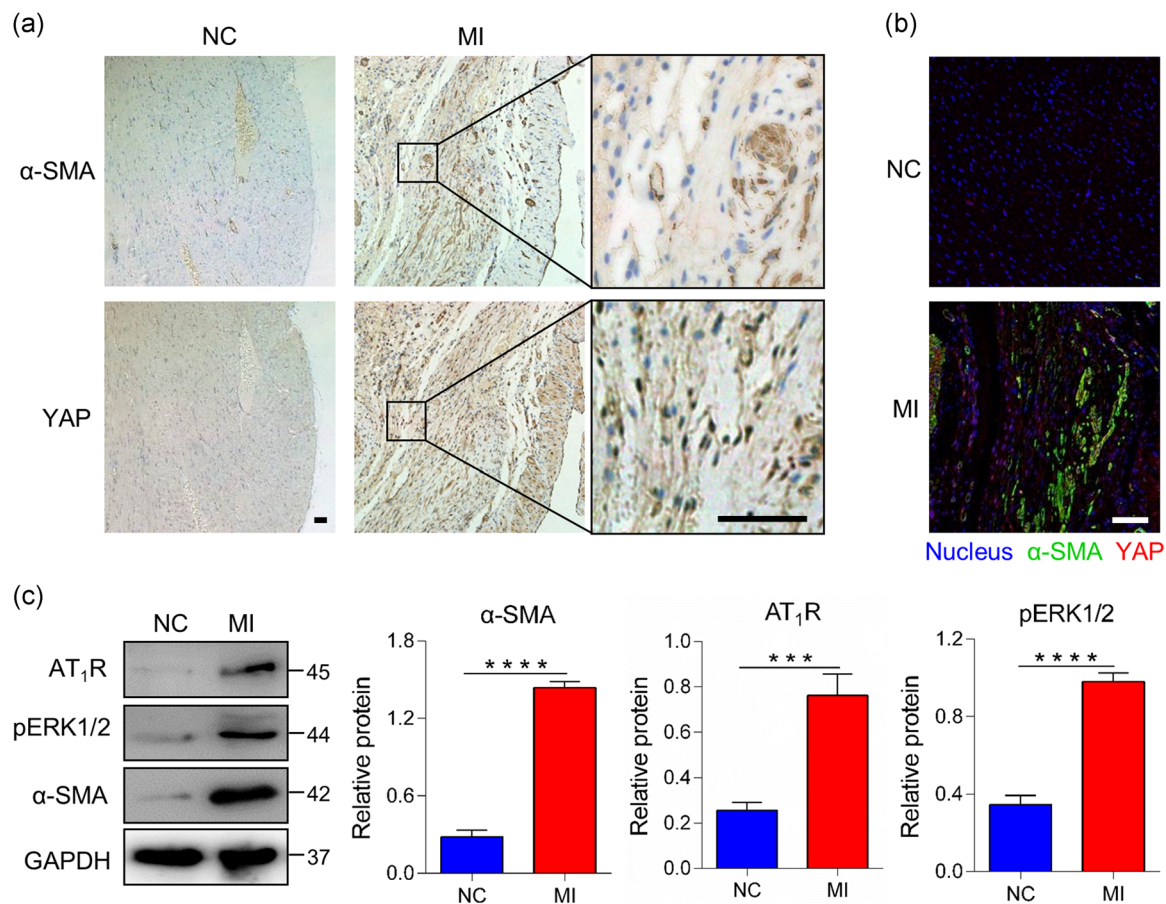

FIGURE 1 YAP was highly expressed in rat MI models. (a) Immunohistochemical staining of α-SMA and YAP expression in the cardiac tissues of the NC and MI rats. Tissues were stained with 3,3′-diaminobenzidine (brown) and counterstained with hematoxylin (blue). (b) Immunofluorescence analysis of YAP (red), α-SMA (green), and nuclei (blue) in the cardiac tissues of the NC and MI rats. Scale bar = 50 μm. (c) Relative protein levels of α-SMA, AT$_1$R, and pERK1/2 determined by Western blot analyses. AT$_1$R, angiotensin II type 1 receptor; ERK1/2, extracellular signal-regulated kinase 1/2; MI, myocardial infarction; NC, normal control; YAP, Yes-associated protein; α-SMA, α-smooth muscle actin

significant difference among the gelatin hydrogels with different stiffnesses (Figure S2b,c). In combination, these results demonstrated that we can generate gelatin hydrogels with different stiffnesses but similar water absorption ratios and degradability without changing the gelatin concentration.

We then cultured rat CFs on gelatin hydrogels with different stiffnesses (4 and 36 kPa), with CFs cultured on cell culture plates as a control. First, we used vimentin as a maker of the CFs. We confirmed that almost all isolated cells displayed vimentin expression, indicating the presence of only CFs (Figure S3). Then, we found that the proliferative ability of the CFs cultured on substrates with different stiffnesses decreased with time but was higher on soft matrix

on Day 7 (Figure S4). Through immunofluorescence staining, we found that different hydrogel stiffnesses imposed different degrees of CF activation, where the expression of α-SMA increased with increasing matrix stiffness (Figure 2a). Moreover, the total expression and nuclear localization of YAP in the CFs significantly increased on the stiff matrix (Figure 2b,c). The higher expression levels of α-SMA and nuclear YAP of the CFs on the stiff matrix than those on the soft matrix were further confirmed by Western blot analyses (Figure 2d) and gene expression analysis (Figure 2e). The consequences of YAP activation on YAP transcriptional targets (CYR61 and CTGF) were confirmed by RT-PCR (Figure S5a). We also confirmed the enhanced expression of other activation markers (Col I, TGF-β1, TCF21, and
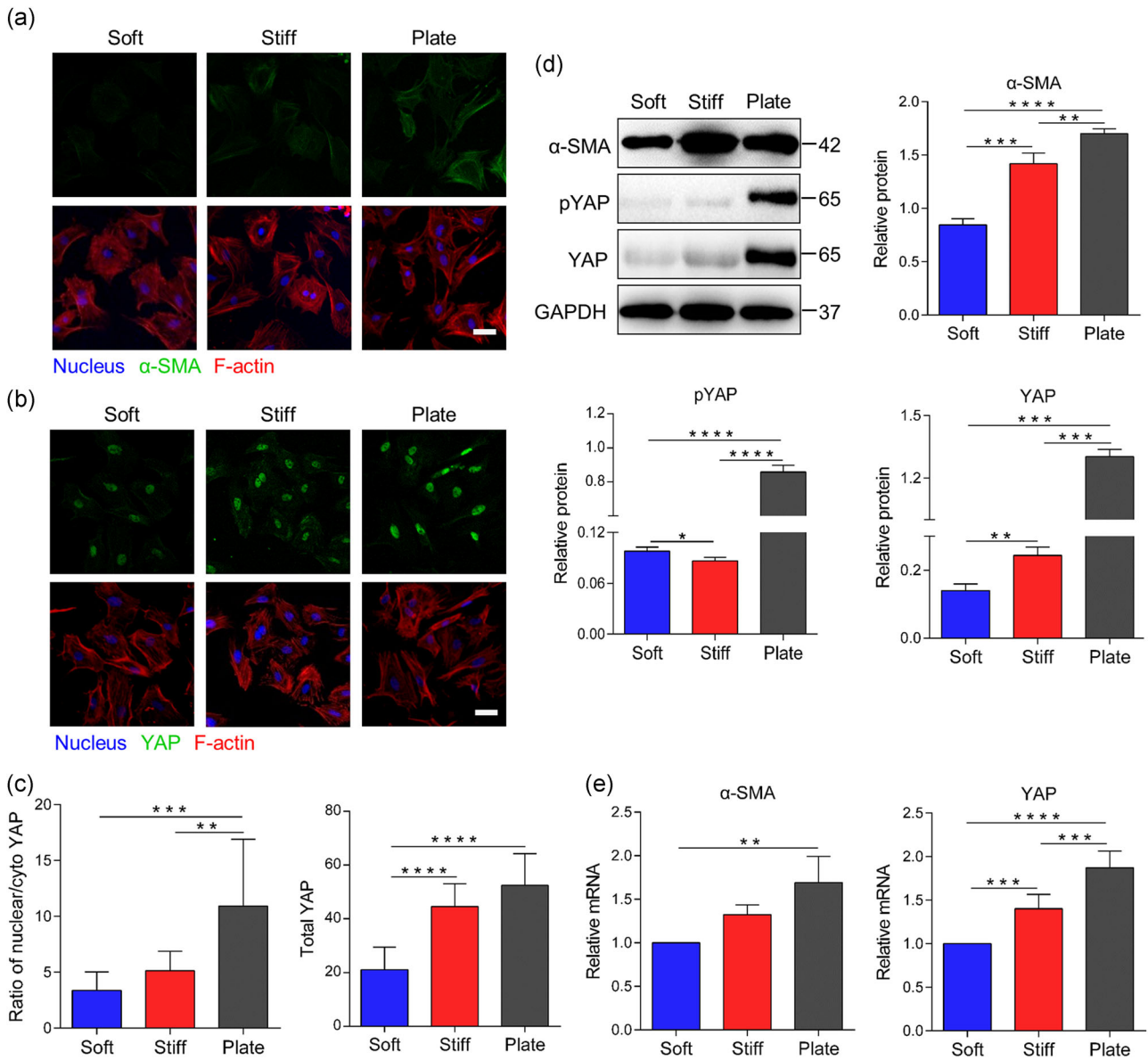
FIGURE 2 The expression and nuclear localization of YAP increased in the CFs cultured on a stiff matrix. (a) Immunofluorescence analysis indicated the differentiation of CFs increased with increasing stiffness (blue, nucleus; green, α-SMA; red, F-actin). Scale bar = 50 μm. (b) Immunofluorescence analysis indicated nuclear YAP increased with increasing stiffness (blue, nucleus; green, YAP; red, F-actin). Scale bar = 50 μm. (c) Quantification of the ratio of nuclear YAP to cytoplasmic YAP and the expression of total YAP in the CFs. (d) The Relative protein levels of α-SMA, pYAP, and YAP determined by Western blot analyses in CFs after 7 days of culture. (e) qRT-PCR analysis of α-SMA and YAP in CFs after 7 days of culture. CF, cardiac fibroblast; YAP, Yes-associated protein; α-SMA, α-smooth muscle actin

PDGFR-α) in the CFs cultured on the stiff matrix (Figure S5b). Collectively, these data indicate that the activity and subcellular localization of YAP could be associated with stiff matrix-induced CF activation.

3.3 | YAP was required for matrix stiffness-mediated CF activation

To evaluate the role of YAP in matrix stiffness-mediated CF activation, we first performed siRNA-mediated knockdown of YAP in the CFs cultured on gelatin hydrogels with different stiffnesses. YAP knockdown efficiency was confirmed at both the mRNA and protein levels (Figure S6a,b). Immunofluorescence staining results showed that YAP-deficient CFs cultured on both soft and stiff matrices had lower expression of α-SMA than the CFs in the control group (Figure 3a). Western blot and PCR analyses also confirmed the decreased α-SMA expression in the YAP-deficient CFs (Figure 3b,c). Moreover, YAP knockdown reduced the expression of other activation markers (Col I, TGF-β1, TCF21, and PDGFR-α; Figure S7). In addition, YAP knockdown reduced the proliferation of the CFs cultured on both soft and stiff matrix (Figure S8). Collectively, these observations suggest that YAP is required for matrix stiffness-mediated CF activation.

To further assess the role of YAP overexpression in the matrix stiffness-mediated fibrogenic response of CFs, we overexpressed YAP in the cultured CFs by cloning full-length YAP from rat CFs into the pEX vector (Figure S9a,b). The immunofluorescence staining results showed that the YAP-overexpressing CFs cultured on both soft and stiff matrices increased the expression of α-SMA compared with CFs in the control group (Figure 4a), which was also confirmed by Western blot and PCR analyses (Figure 4b,c). We then confirmed that the expression of other activation markers (Col I, TGF-β1, TCF21, and PDGFR-α) was increased in the YAP-overexpressing CFs (Figure S10). Moreover, YAP overexpression increased the proliferation of the CFs cultured on both the soft and stiff gelatin hydrogels compared with CFs in the control group (Figure S11). These observations confirmed that YAP overexpression could promote the fibrogenic response of CFs.

3.4 | YAP was downstream of AT$_1$R to control CF activation

We have previously demonstrated that AT$_1$R plays a critical role in sensing matrix stiffness to regulate CF activation (Yong et al., 2016). Here, to uncover the relationship between YAP and AT$_1$R in mediating matrix stiffness-regulated CF activation, we used LP (an AT$_1$R inhibitor) to block AT$_1$R-mediated signaling of the CFs cultured on
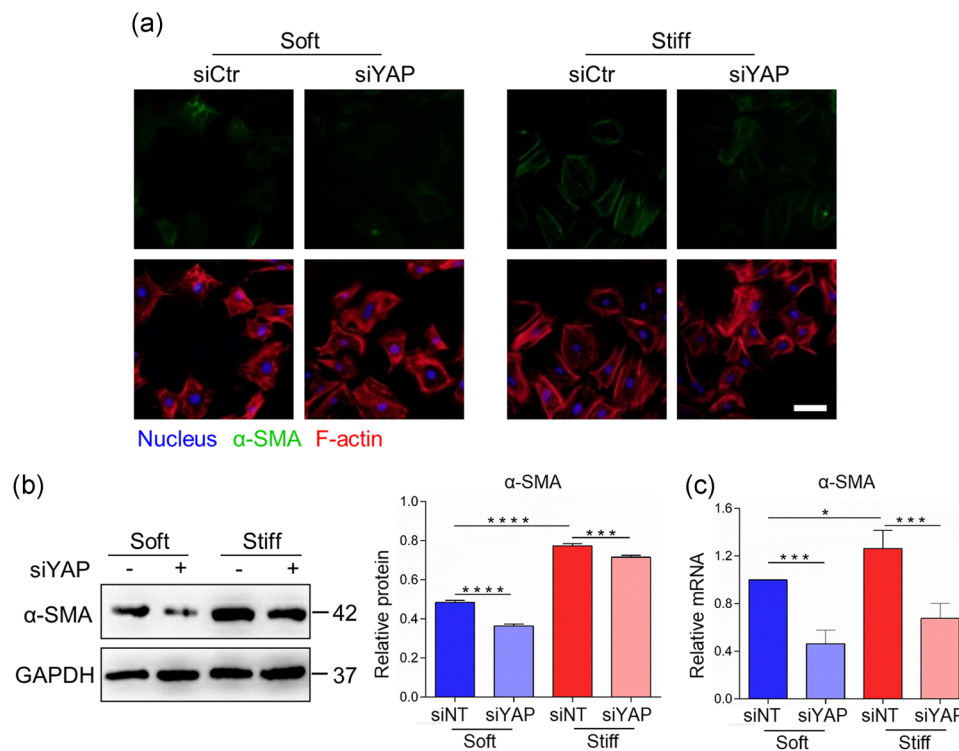
FIGURE 3 YAP was required for stiff matrix-induced CF activation. (a) Immunofluorescence analysis indicated that the differentiation of CFs decreased when transfected with siRNAs targeting YAP (blue, nucleus; green, α-SMA; red, F-actin). Scale bar = 50 μm. (b) The relative protein levels of α-SMA determined by Western blot when the CFs were transfected with siRNAs targeting YAP after 3 days of culture. (c) qRT-PCR analysis of α-SMA when the CFs were transfected with siRNAs targeting YAP. CF, cardiac fibroblast; Ctr, control; GAPDH, glyceraldehyde-3-phosphate dehydrogenase; qRT-PCR, quantitative real-time polymerase chain reaction; siRNA, small interfering RNA; YAP, Yes-associated protein; α-SMA, α-smooth muscle actin
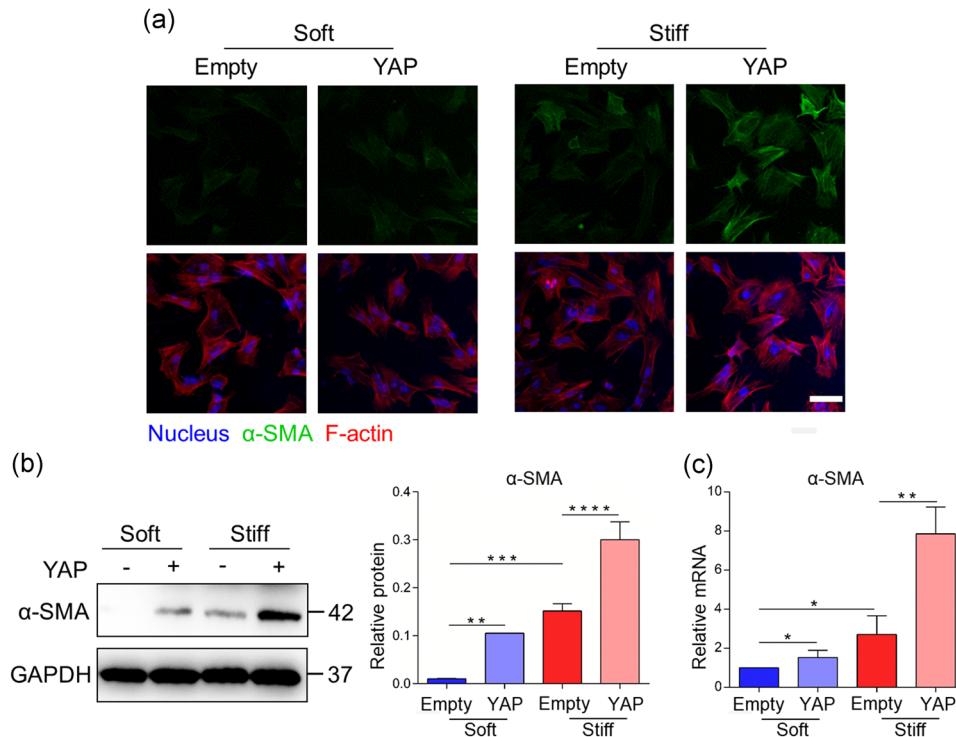
FIGURE 4 YAP overexpression promoted fibrogenic response of CFs. (a) Immunofluorescence analysis indicated that the differentiation of CFs increased when transfected with YAP (blue, nucleus; green, α-SMA; red, F-actin). Scale bar = 50 μm. (b) The relative protein levels of α-SMA determined by Western blot when the CFs were transfected with YAP after 3 days of culture. (c) qRT-PCR analysis of α-SMA when the CFs were transfected with YAP. CF, cardiac fibroblast; GAPDH, glyceraldehyde-3-phosphate dehydrogenase; qRT-PCR, quantitative real-time polymerase chain reaction; YAP, Yes-associated protein; α-SMA, α-smooth muscle actin

the soft and stiff matrices. Through immunofluorescence staining, we observed that α-SMA expression in the CFs was reduced in the presence of LP (Figure 5a). Moreover, LP significantly inhibited the nuclear localization and total expression of YAP (Figure 5b,c). Western blot and PCR analyses further confirmed that blocking AT_1R decreased the expression levels of α-SMA and YAP, whereas increasing the expression levels of pYAP (Figure 5d,e). These results imply that AT_1R may function as an important upstream molecule that mediates YAP-dependent CF mechanotransduction.

To determine whether YAP is downstream of AT_1R in mediating matrix stiffness-regulated CF activation, we overexpressed YAP in CFs cultured on gelatin hydrogels with different stiffnesses and confirmed the overexpression by Western blot (Figure 6b), and LP was added as an antagonist of AT_1R at the same time. The immunofluorescence staining results showed that the YAP-overexpressing CFs displayed higher expression levels of α-SMA than the control CFs even in the presence of LP (Figure 6a), and these results were further confirmed by Western blot and PCR analyses (Figure 6b,c). These observations confirmed that YAP is downstream of AT_1R in mediating matrix stiffness-regulated CF activation.

4 | DISCUSSION

CFs have been found to activate into myofibroblasts after MI, promoting the development of stromal fibrosis and scaring in the failing heart (Suurmeijer et al., 2003). Accordingly, the matrix stiffness in the pathological myocardium significantly increases and has been found to function both independently and cooperatively with biochemical cues to promote CF activation and thus fibrosis development (Fan, Takawale, Lee, & Kassiri, 2012; Bourhis et al., 2013). The stiffness of living tissues varies over several orders of magnitude (Albers et al., 2011; Engler et al., 2004; Georges et al., 2007; Hinz, 2013; Ho et al., 2010; Ho, Marshall, Ryder, & Marshall, 2007). However, the mechanical microenvironment of cells cultured in vitro is highly nonphysiological, given the high stiffness of the cell culture plate (~GPa). This issue raises concerns that many physiological phenomena are attributed to the baseline behavior of cultured cells, which may be artificial (Wells, 2010). Various materials have been developed for studying cell mechanical responses in vitro by mimicking physiological conditions. For instance, hydrogels, including polyacrylamide, collagen, and fibrin can provide different culture conditions of physiological stiffness (Huang et al., 2017). Here, we used gelatin hydrogels for their highly variable stiffness and good biocompatibility (McCain, Agarwal, Nesmith, Nesmith, & Parker, 2014). This study first verified the effect of matrix stiffness on CF phenotype transformation, *that is*, increasing matrix stiffness promotes α-SMA expression (Figure 2a). This finding is consistent with previous reports from other types of cells such as hepatic stellate cells (Caliari et al., 2016; Guvendiren, Perepelyuk, Wells, & Burdick, 2014), mesenchymal stem cells (Guvendiren &
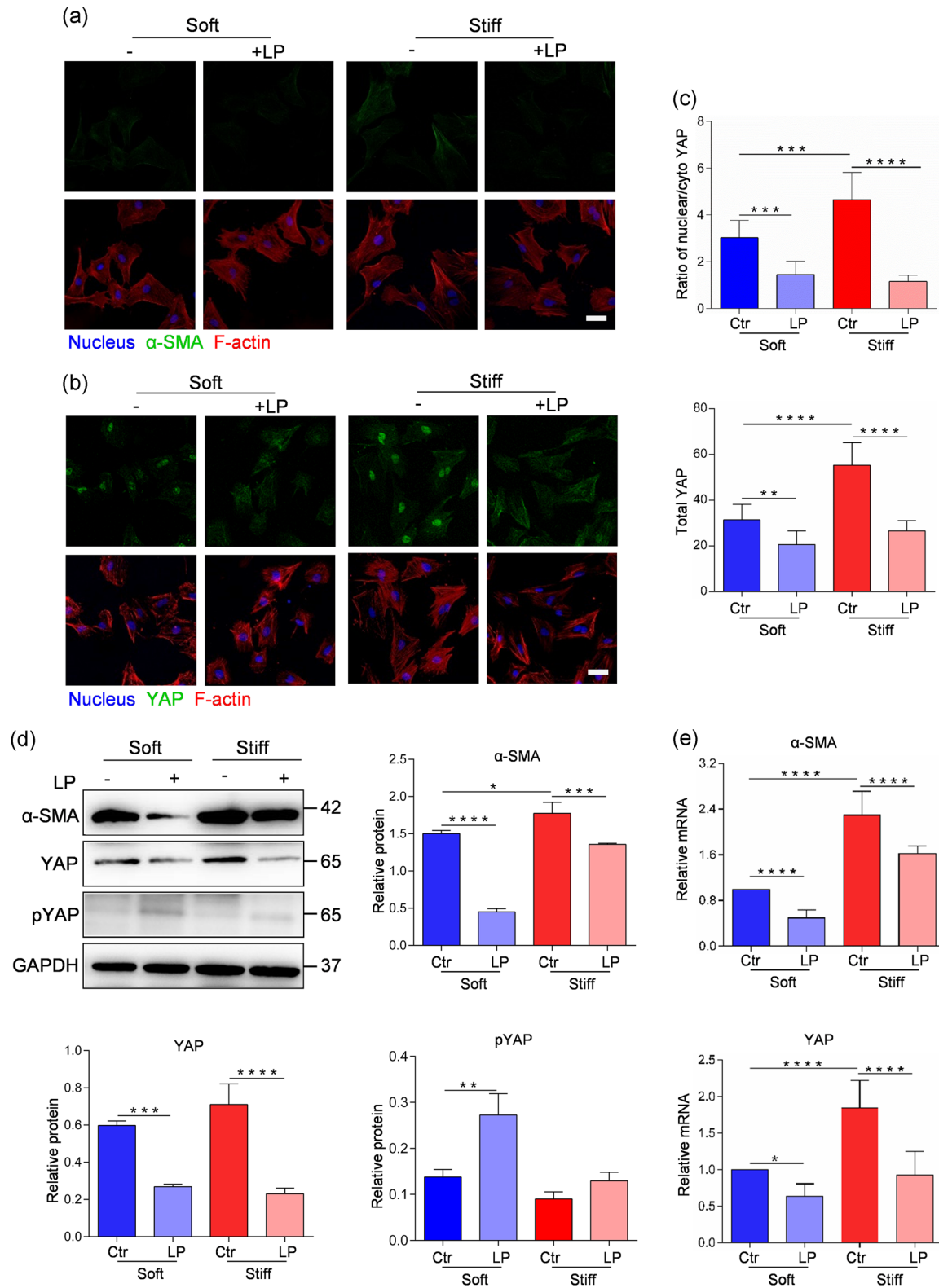
FIGURE 5 The expression of YAP and α-SMA in CFs were regulated by AT$_1$R. (a) Immunofluorescence analysis indicated that the differentiation of CFs decreased with the addition of LP (blue, nucleus; green, α-SMA; red, F-actin). Scale bar = 50 μm. (b) Immunofluorescence analysis indicated that nuclear YAP in CFs decreased with the addition of LP (blue, nucleus; green, YAP; red, F-actin). Scale bar = 50 μm. (c) Quantification of the ratio of nuclear YAP to cytoplasmic YAP and the expression of total YAP in CFs. (d) The Relative protein levels of α-SMA, YAP and pYAP determined by Western blot analyses in CFs after 7 days of culture. (e) qRT-PCR analysis of α-SMA and YAP in CFs decreased with the addition of LP after 7 days of culture. AT$_1$R, angiotensin II type 1 receptor; CF, cardiac fibroblast; Ctr, control; GAPDH, glyceraldehyde-3-phosphate dehydrogenase; LP, losartan potassium; YAP, Yes-associated protein; α-SMA, α-smooth muscle actin
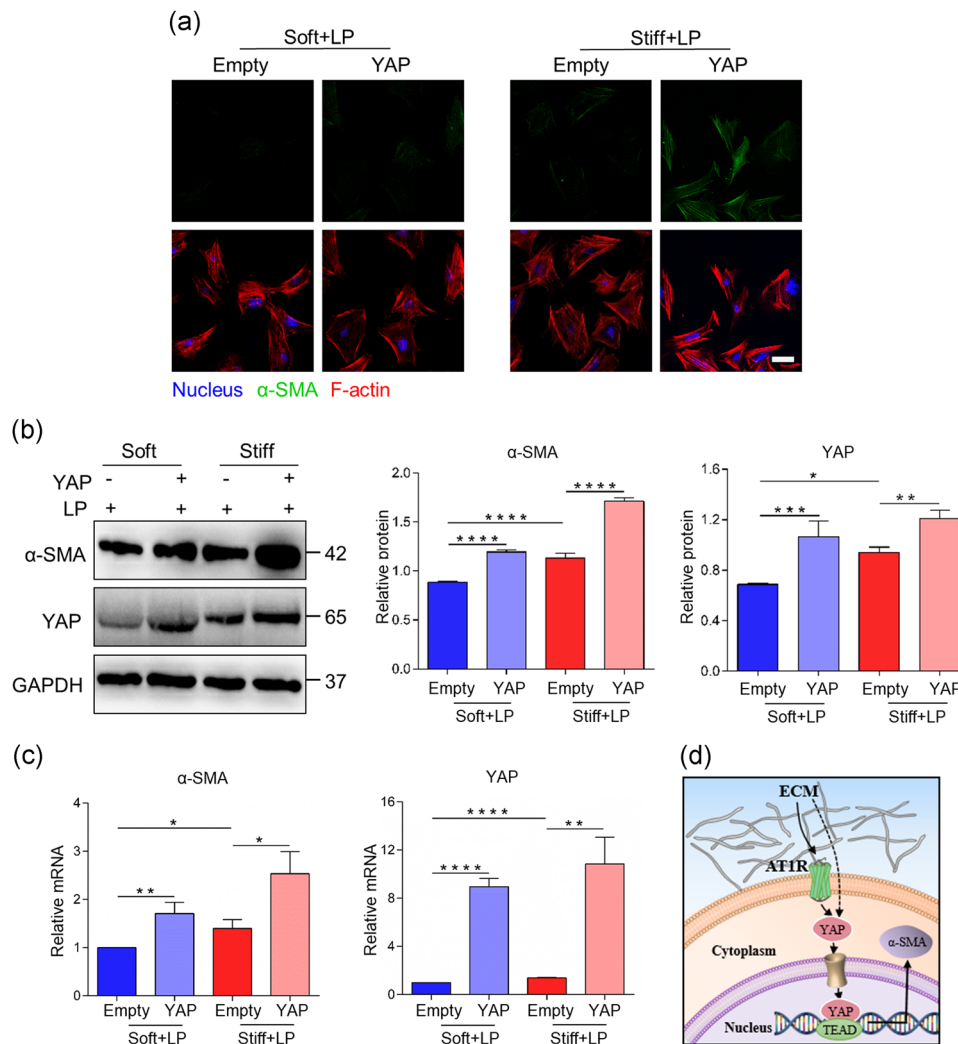
FIGURE 6 YAP was downstream of AT$_1$R to control CF activation. (a) Immunofluorescence analysis indicated that the differentiation of CFs decreased after being transfected with YAP and was suppressed by LP (blue, nucleus; green, a-SMA; red, F-actin). Scale bar = 50 μm. (b) The relative protein levels of α-SMA and YAP determined by Western blot. (c) qRT-PCR analysis of α-SMA and YAP. (d) Schematic depicting how matrix stiffness regulates YAP via AT$_1$R to control CF differentiation. AT$_1$R, angiotensin II type 1 receptor; CF, cardiac fibroblast; GAPDH, glyceraldehyde-3-phosphate dehydrogenase; LP, losartan potassium; YAP, Yes-associated protein; α-SMA, α-smooth muscle actin

Burdick, 2011), and NIH 3T3 fibroblasts (Ondeck & Engler, 2016). Compared with the reported results in the literature, our work showed that the CFs cultured on the soft gelatin hydrogels had nonnegligible increases in expression of α-SMA (Figure 2d). We suspect that this change may be due to the presence of abundant adhesion ligands in the gelatin hydrogels (Czerner, Fellay, Suárez, Frontini, & Fasce, 2015; Kathuria, Tripathi, Kar, & Kumar, 2009).

Although matrix stiffness has been shown to mediate fibroblast phenotypic transformation (Olsen et al., 2011; Huang et al., 2012), the underlying mechanoregulatory pathways are still poorly understood. Here, we demonstrated, for the first time, a new role for YAP as a mechanotransducer in cardiac fibrosis. Classically believed to be a target of the Hippo pathway, YAP is regulated by phosphorylation of serine residues, which not only controls their intracellular localization but also controls their ubiquitination and subsequent degradation (Zhao et al., 2010). An important discovery in 2011

showed that YAP could also be regulated by matrix stiffness and cell shape (Dupont et al., 2011). Since then, YAP has been found to transduce various mechanical cues in controlling cell growth, migration, and differentiation (Aragona et al., 2013; Nakajima et al., 2017; Nardone et al., 2017). We showed that the enhanced activation of CFs on the stiff matrix was mediated through the enhanced expression and nuclear localization of YAP (Figure 2b). Consistent with this finding, others reports have also noted that YAP was activated in some diseases (e.g., Dupuytren disease; Piersma et al., 2015). The underlying mechanisms of this mechanical regulation of YAP are unclear, although both Hippo-dependent and Hippo-independent pathways may contribute (Aragona et al., 2013; Codelia, Sun, & Irvine, 2014; Rauskolb, Sun, Sun, Pan, & Irvine, 2014). Whether the pathway activity of CF activation is regulated by other mechanical signaling molecules remains an open question worthy of further exploration.

Recognizing the importance of YAP in cardiac fibrosis, we further demonstrated that AT$_1$R, as a GPCR widely expressed in various types of cells including CFs and cardiomyocytes, mediated matrix stiffness-induced CF activation through YAP. The activation of AT$_1$R was shown to be regulated either by angiotensin II, endogenous agonist, or by biomechanical stress (Schnitzler et al., 2008; Zou et al., 2004). Here, we found that AT$_1$R, activated by matrix stiffness and as an upstream mechanical signaling molecule, regulated the transcriptional activator YAP to promote cardiac fibrosis (Figures 5b,c and 6a). Our results also revealed that AT$_1$R can only regulate YAP to a certain extent (Figure 5b,d). The reason may be that AT$_1$R, as an upstream factor, can also simultaneously activate other downstream signaling pathways (e.g., mitogen-activated protein kinase pathways, the ERK1/2 and JNK3 pathways; Tilley, 2011; Tohgo, Pierce, Choy, Lefkowitz, & Luttrell, 2002; Song, Coffa, Fu, & Gurevich, 2009).

YAP as a mechanical transducer has not been widely studied in the activation of CFs as it has been in other cells. Since the mechanism by which YAP activation is regulated is not well understood, drugs that use YAP as a single target can only be used to slow the disease. For example, YAP activation, a critical driver of hepatic stellate cell activation, can cause liver fibrosis, while the use of verteporfin (VP, a pharmacological inhibitor of YAP) presents a novel approach for treating liver fibrosis by reducing fibrogenesis (Mannaerts et al., 2015). In clinical and preclinical studies of some diseases, AT$_1$R-related signaling pathways have emerged as promising therapeutic targets. For instance, studies have shown that blocking AT$_1$R may limit the inflammatory nature of immune responses in the heart, and early use of angiotensin receptor blockers in Duchenne muscular dystrophy patients could limit myocardial damage and subsequent cardiomyopathy (Meyers et al., 2019). More important, we found that blocking AT$_1$R with LP can limit the activation of CFs and decrease the expression and nuclear location of YAP (Figure 5a,b). Further studies based on animal models (e.g., knockouts and transgenic models) with a specific focus on assessing CFs (Kaur et al., 2016; Sava et al., 2017), as well as studies using specific YAP and AT$_1$R inhibitors, are necessary to better understand the roles of YAP and AT$_1$R in mechanically regulated CF activation and cardiac fibrosis. A key barrier to the development of effective anti-fibrotic therapies is the complexity and redundancy of the fibrotic signaling network. An underrecognized contributor to this complexity is the synergistic interaction between biochemical and mechanical regulatory signals. As the development of cardiac fibrosis is an important factor in many cardiovascular diseases leading to severe heart failure, the development of new therapies focused on regulating YAP and YAP-related pathways may provide new therapies that can beneficially alter the cardiac remodeling process. Many new studies are needed for this purpose.

5 | CONCLUSIONS

In this study, high expression and transferring into the nucleus of YAP in the pathological region was confirmed by constructing an MI rat model in vivo, and AT$_1$R was shown to be highly expressed and activated in the pathological region. Then, we constructed a matrix stiffness-mediated myocardial fibrosis model in vitro for mechanism studies. Our results identified an important role of YAP in mediating matrix stiffness-induced CF activation after YAP knockout and overexpressed in the CFs. We also established the YAP pathway as an important signaling branch downstream of AT$_1$R in CF mechanotransduction. This study may help to better understand the mechanism of fibrotic mechanotransduction and inspire the development of new approaches for treating cardiac fibrosis in the future.

AUTHOUR CONTRIBUTIONS

L. N., G. H., and F. X. designed the experiments. L. N., Y. J., and M. W. conducted cell and molecular experiments. Y. W., L. N., Y. F., D. G. and Y. J. carried out animal experiments. L. N., G. H., H. L., and X. Z. analyzed the data. H. L. and Y. H. helped with figure edition. L. N. and G. H. wrote the manuscript. All authors edited the manuscript.

DATA AVAILABILITY STATEMENT

All data generated or analyzed during the study are included in this article and its supplementary materials.

ORCID

Guoyou Huang (ID) http://orcid.org/0000-0002-0369-877X

REFERENCES

Albers, E. L., Pugh, M. E., Hill, K. D., Li, W., Loyd, J. E., & Doyle, T. P. (2011). Percutaneous vascular stent implantation as treatment for central vascular obstruction due to fibrosing mediastinitis. *Circulation*, 123(13), 1391–1399.

Aragona, M., Panciera, T., Manfrin, A., Giulitti, S., Michielin, F., Elvassore, N., ... Piccolo, S. (2013). A mechanical checkpoint controls multicellular growth through YAP/TAZ regulation by actin-processing factors. *Cell*, 154(5), 1047–1059.

Bourhis, J. M., Vadon-Le Goff, S., Afrache, H., Mariano, N., Kronenberg, D., Thielens, N., ... Hulmes, D. J. S. (2013). Procollagen C-proteinase enhancer grasps the stalk of the C-propeptide trimer to boost collagen precursor maturation. *Proceedings of the National Academy of Sciences of the United States of America*, 110(16), 6394–6399.

Bryant, C. E., Gay, N. J., Heymans, S., Sacre, S., Schaefer, L., & Midwood, K. S. (2015). Advances in Toll-like receptor biology: Modes of activation by diverse stimuli. *CRC Critical Reviews in Biochemistry*, 50(5), 359–379.

Caliari, S. R., Perepelyuk, M., Cosgrove, B. D., Tsai, S. J., Lee, G. Y., Mauck, R. L., ... Burdick, J. A. (2016). Stiffening hydrogels for investigating the dynamics of hepatic stellate cell mechanotransduction during myofibroblast activation. *Scientific Reports*, 6(1), 21387.

Calvo, F., Ege, N., Grande-Garcia, A., Hooper, S., Jenkins, R. P., Chaudhry, S. I., ... Sahai, E. (2013). Mechanotransduction and

YAP-dependent matrix remodelling is required for the generation and maintenance of cancer-associated fibroblasts. *Nature Cell Biology*, *15*(6), 637–646.

Codelia, V. A., Sun, G., & Irvine, K. D. (2014). Regulation of YAP by mechanical strain through Jnk and Hippo signaling. *Current Biology*, *24*(17), 2012-2017.

Couchman, J. R. (2010). Transmembrane signaling proteoglycans. *Annual Review of Cell and Developmental Biology*, *26*(1), 89–114.

Czerner, M., Fellay, L. S., Suárez, M. P., Frontini, P. M., & Fasce, L. A. (2015). Determination of elastic modulus of gelatin gels by indentation experiments. *Procedia Materials Science*, *8*, 287–296.

Dupont, S., Morsut, L., Aragona, M., Enzo, E., Giulitti, S., Cordenonsi, M., … Piccolo, S. (2011). Role of YAP/TAZ in mechanotransduction. *Nature*, *474*(7350), 179–183.

Engler, A. J., Carag-Krieger, C., Johnson, C. P., Raab, M., Tang, H. Y., Speicher, D. W., … Discher, D. E. (2008). Embryonic cardiomyocytes beat best on a matrix with heart-like elasticity: Scar-like rigidity inhibits beating. *Journal of Cell Science*, *121*(Pt22), 3794-3802.

Engler, A. J., Griffin, M. A., Sen, S., Bönnemann, C. G., Sweeney, H. L., & Discher, D. E. (2004). Myotubes differentiate optimally on substrates with tissue-like stiffness: Pathological implications for soft or stiff microenvironments. *Journal of Cell Biology*, *166*(6), 877–887.

Fan, D., Takawale, A., Lee, J., & Kassiri, Z. (2012). Cardiac fibroblasts, fibrosis and extracellular matrix remodeling in heart disease. *Fibrogenesis & Tissue Repair*, *5*(1), 15.

Flevaris, P., Khan, S. S., Eren, M., Schuldt, A. J. T., Shah, S. J., Lee, D. C., … Ghosh, A. K. (2017). Plasminogen activator inhibitor type I controls cardiomyocyte transforming growth factor-β and cardiac fibrosis. *Circulation*, *136*(7), 664-679.

Frankenreiter, S., Bednarczyk, P., Kniess, A., Bork, N., Straubinger, J., Koprowski, P., … Murphy, M. P. (2017). cGMP-elevating compounds and ischemic conditioning provide cardioprotection against ischemia and reperfusion injury via cardiomyocyte-specific BK channels. *Circulation*, *136*(24), 2237–2335.

Galie, P. A., Westfall, M. V., & Stegemann, J. P. (2011). Reduced serum content and increased matrix stiffness promote the cardiac myofibroblast transition in 3D collagen matrices. *Cardiovascular Pathology*, *20*(6), 325–333.

Georges, P. C., Hui, J. J., Gombos, Z., Mccormick, M. E., Wang, A. Y., Uemura, M., … Wells, R. G. (2007). Increased stiffness of the rat liver precedes matrix deposition: Implications for fibrosis. *American Journal of Physiology—Gastrointestinal and Liver Physiology*, *293*(6), 1147–1154.

Guvendiren, M., & Burdick, J. A. (2011). Stiffening hydrogels to probe short- and long-term cellular responses to dynamic mechanics. *Nature Communications*, *3*(4), 792.

Guvendiren, M., Perepelyuk, M., Wells, R. G., & Burdick, J. A. (2014). Hydrogels with differential and patterned mechanics to study stiffness-mediated myofibroblastic differentiation of hepatic stellate cells. *Journal of the Mechanical Behavior of Biomedical Materials*, *38*(4), 198–208.

Hale, T. M. (2016). Persistent phenotypic shift in cardiac fibroblasts: Impact of transient renin angiotensin system inhibition. *Journal of Molecular & Cellular Cardiology*, *93*, 125–132.

Herum, K. M., Choppe, J., Kumar, A., Engler, A. J., & Mcculloch, A. D. (2017). Mechanical regulation of cardiac fibroblast pro-fibrotic phenotypes. *Molecular Biology of the Cell*, *28*(14), 1871–1882.

Herum, K. M., Lunde, I. G., McCulloch, A. D., & Christensen, G. (2017). The soft-and hard-heartedness of cardiac fibroblasts: Mechanotransduction signaling pathways in fibrosis of the heart. *Journal of Clinical Medicine*, *6*(5), E53.

Hinz, B. (2013). Matrix mechanics and regulation of the fibroblast phenotype. *Periodontology*, *63*(1), 14–28.

Hinz, B., & Lagares, D. (2020). Evasion of apoptosis by myofibroblasts: A hallmark of fibrotic diseases. *Nature Reviews Rheumatology*, *16*(1), 11–31.

Ho, S. P., Kurylo, M. P., Fong, T. K., Lee, S. S. J., Wagner, H. D., Ryder, M. I., & Marshall, G. W. (2010). The biomechanical characteristics of the bone-periodontal ligament-cementum complex. *Biomaterials*, *31*(25), 6635–6646.

Ho, S. P., Marshall, S. J., Ryder, M. I., & Marshall, G. W. (2007). The tooth attachment mechanism defined by structure, chemical composition and mechanical properties of collagen fibers in the periodontium. *Biomaterials*, *28*(35), 5238–5245.

Hu, J. K., Du, W., Shelton, S. J., Oldham, M. C., DiPersio, C. M., & Klein, O. D. (2017). An FAK-YAP-mTOR signaling axis regulates stem cell-based tissue renewal in mice. *Cell Stem Cell*, *21*(1), 91–106.

Huang, G., Li, F., Zhao, X., Ma, Y., Li, Y., Lin, M., … Xu, F. (2017). Functional and biomimetic materials for engineering of the three-dimensional cell microenvironment. *Chemical Reviews*, *117*(20), 12764–12850.

Huang, X., Yang, N., Fiore, V. F., Barker, T. H., Sun, Y., Morris, S. W., & Zhou, Y. (2012). Matrix stiffness-induced myofibroblast differentiation is mediated by intrinsic mechanotransduction. *American Journal of Respiratory Cell & Molecular Biology*, *47*(3), 340–348.

Kathuria, N., Tripathi, A., Kar, K. K., & Kumar, A. (2009). Synthesis and characterization of elastic and macroporous chitosan–gelatin cryogels for tissue engineering. *Acta Biomaterialia*, *5*(1), 406–418.

Kaur, H., Takefuji, M., Ngai, C. Y., Carvalho, J., Bayer, J., Wietelmann, A., … Wettschureck, N. (2016). Targeted ablation of periostin-expressing activated fibroblasts prevents adverse cardiac remodeling in mice. *Circulation Research*, *118*(12), 1906–1917.

Kong, M., Lee, J., Yazdi, I. K., Miri, A. K., Lin, Y.-D., Seo, J., & Shin, S. R. (2019). Cardiac fibrotic remodeling on a chip with dynamic mechanical stimulation. *Advanced Healthcare Materials*, *8*(3), e1801146.

Lagares, D., San tos, A., Grasberger, P. E., Liu, F., Probst, C. K., Rahimi, R. A., … Bhola, P. (2017). Targeted apoptosis of myofibroblasts with the BH3 mimetic ABT-263 reverses established fibrosis. *Science Translational Medicine*, *9*(420), eaal3765.

Lee, S., Serpooshan, V., Tong, X., Venkatraman, S., Lee, M., Lee, J., … Yang, F. (2017). Contractile force generation by 3D hiPSC-derived cardiac tissues is enhanced by rapid establishment of cellular interconnection in matrix with muscle-mimicking stiffness. *Biomaterials*, *131*, 111–120.

Liu, F., Lagares, D., Choi, K. M., Stopfer, L., Marinkovic, A., Vrbanac, V., … Tschumperlin, D. J. (2015). Mechanosignaling through YAP and TAZ drives fibroblast activation and fibrosis. *American Journal of Physiology-Lung Cellular and Molecular Physiology*, *308*(4), 344–357.

Low, B. C., Pan, C. Q., Shivashankar, G. V., Bershadsky, A., Sudol, M., & Sheetz, M. (2014). YAP/TAZ as mechanosensors and mechanotransducers in regulating organ size and tumor growth. *FEBS Letters*, *588*(16), 2663–2670.

Makino, A., & Schmid-Schönbein, G. W. (2006). G-Protein coupled membrane receptors may serve as mechanosensors for fluid shear stress in neutrophils. *American Journal of Physiology: Cell Physiology*, *290*(6), 1633–1639.

Mannaerts, I., Leite, S. B., Verhulst, S., Claerhout, S., Eysackers, N., Thoen, L. F. R., … van Grunsven, L. A. (2015). The Hippo pathway effector YAP controls mouse hepatic stellate cell activation. *Journal of Hepatology*, *63*(3), 679–688.

McCain, M. L., Agarwal, A., Nesmith, H. W., Nesmith, A. P., & Parker, K. K. (2014). Micromolded gelatin hydrogels for extended culture of engineered cardiac tissues. *Biomaterials*, *35*(21), 5462–5471.

Meyers, T. A., Heitzman, J. A., Krebsbach, A. M., Aufdembrink, L. M., Hughes, R., Bartolomucci, A., & Townsend, D. (2019). Acute AT1R blockade prevents isoproterenol-induced injury in mdx hearts. *Journal of Molecular and Cellular Cardiology*, *128*, 51–61.

Morine, K. J., Qiao, X., York, S., Natov, P. S., Paruchuri, V., Zhang, Y., ... Kapur, N. K. (2018). Bone morphogenetic protein 9 reduces cardiac fibrosis and improves cardiac function in heart failure. *Circulation*, *138*(5), 513–526.

Mouillerson, S., Langer, C., Guettler, S., Mcdonald, N. Q., & Treisman, R. (2011). Structure of a pentavalent G-actin*MRTF-A complex reveals how G-actin controls nucleocytoplasmic shuttling of a transcriptional coactivator. *Science Signaling*, *4*(177), ra40.

Mouton, A. J., Ma, Y., Gonzalez, O. J. R., Daseke, M. J., Flynn, E. R., Freeman, T. C., ... Lindsey, M. L. (2019). Fibroblast polarization over the myocardial infarction time continuum shifts roles from inflammation to angiogenesis. *Basic Research in Cardiology*, *114*(2), 6.

Nakajima, H., Yamamoto, K., Agarwala, S., Terai, K., Fukui, H., Fukuhara, S., ... Schmelzer, E. (2017). Flow-dependent endothelial YAP regulation contributes to vessel maintenance. *Developmental Cell*, *40*(6), 523-536.

Nardone, G., Oliver-De La Cruz, J., Vrbsky, J., Martini, C., Pribyl, J., Skládal, P., ... Forte, G. (2017). YAP regulates cell mechanics by controlling focal adhesion assembly. *Nature Communications*, *8*, 15321.

Olsen, A. L., Bloomer, S. A., Chan, E. P., Ga?A, M. D. A., Georges, P. C., Bridget, S., ... Wells, R. G. (2011). Hepatic stellate cells require a stiff environment for myofibroblastic differentiation. *American Journal of Physiology. Gastrointestinal and Liver Physiology*, *301*(1), G110–G118.

Ondeck, M. G., & Engler, A. J. (2016). Mechanical characterization of a dynamic and tunable methacrylated hyaluronic acid hydrogel. *Journal of Biomechanical Engineering*, *138*(2), 021003.

Panciera, T., Azzolin, L., Cordenonsi, M., & Piccolo, S. (2017). Mechanobiology of YAP and TAZ in physiology and disease. *Nature Reviews Molecular Cell Biology*, *18*(12), 758–770.

Park, S., Ranjbarvazirj, S., Lay, F. D., Zhao, P., Miller, M. J., Dhaliwal, J. S., & Soffer, J. M. (2018). Genetic regulation of fibroblast activation and proliferation in cardiac fibrosis. *Circulation*, *42*(3), 1224-1235.

Piersma, B., de Rond, S., Werker, P. M. N., Boo, S., Hinz, B., van Beuge, M. M., & Bank, R. A. (2015). YAP1 Is a driver of myofibroblast differentiation in normal and diseased fibroblasts. *American Journal of Pathology*, *185*(12), 3326–3337.

Rauskolb, C., Sun, S., Sun, G., Pan, Y., & Irvine, D. K. (2014). Cytoskeletal tension inhibits Hippo signaling through an Ajuba-Warts complex. *Cell*, *158*(1), 143–156.

Rinschen, M., Grahammer, F., Huber, T., Benzing, T., & Schermer, B. (2017). Yap-mediated mechanotransduction determines the podocyte's response to damage. *Science Signaling, 10*(474), eaaf8165.

Roduit, C., Van De Goot, G., De Los Rios, P., Yersin, A., Steiner, P., Dietler, G., ... Kasas, S. (2008). Elastic membrane heterogeneity of living cells revealed by stiff nanoscale membrane domains. *Biophysical Journal*, *94*(4), 1521–1532.

Santiago, J. J., Dangerfield, A. L., Rattan, S. G., Bathe, K. L., Cunnington, R. H., Raizman, J. E., ... Dixon, I. M. (2010). Cardiac fibroblast to myofibroblast differentiation in vivo and in vitro: Expression of focal adhesion components in neonatal and adult rat ventricular myofibroblasts. *Developmental Dynamics*, *239*(6), 1573–1584.

Scholz, N., Monk, K. R., Kittel, R. J., & Langenhan, T. (2016). Adhesion GPCRs as a putative class of metabotropic mechanosensors. *Handbook of Experimental Pharmacology*, *234*, 221–247.

Schroeder, M. C., & Halder, G. (2012). Regulation of the Hippo pathway by cell architecture and mechanical signals. *Seminars in Cell & Developmental Biology*, *23*(7), 803–811.

Schnitzler, M. Y., Storch, U., & Gudermann, T. (2011). AT1 receptors as mechanosensors. *Current Opinion in Pharmacology*, *11*(2), 112–116.

Schnitzler, M. M. Y., Storch, U., Meibers, S., Nurwakagari, P., Breit, A., Essin, K., ... Gudermann, T. (2008). Gq-coupled receptors as mechanosensors mediating myogenic vasoconstriction. *EMBO Journal*, *27*(23), 3092–3103.

Song, X., Coffa, S., Fu, H., & Gurevich, V. V. (2009). How does arrestin assemble MAPKs into a signaling complex? *Journal of Biological Chemistry*, *284*(1), 685–695.

Suurmeijer, A. J., Clement, S., Francesconi, A., Bocchi, L., Angelini, A., Van Veldhuisen, D. J., ... Orlandi, A. (2003). Alpha-actin isoform distribution in normal and failing human heart: A morphological, morphometric, and biochemical study. *Journal of Pathology*, *199*(3), 387–397.

Taniguchi, K., Wu, L. W., Grivennikov, S. I., de Jong, P. R., Lian, I., Yu, F. X., ... Karin, M. (2015). A gp130-Src-YAP module links inflammation to epithelial regeneration. *Nature*, *519*(7541), 57–62.

Tilley, D. G. (2011). Functional relevance of biased signaling at the angiotensin II type 1 receptor. *Endocrine, Metabolic & Immune Disorders Drug Targets*, *11*(2), 99–111.

Tohgo, A., Pierce, K. L., Choy, E. W., Lefkowitz, R. J., & Luttrell, L. M. (2002). β-Arrestin scaffolding of the ERK cascade enhances cytosolic ERK activity but inhibits ERK-mediated transcription following angiotensin AT1a receptor stimulation. *Journal of Biological Chemistry*, *277*(11), 9429–9436.

Vadon-Le Goff, S., Kronenberg, D., Bourhis, J., Bijakowski, C., Raynal, N., Ruggiero, F., ... Moali, C. (2011). Procollagen C-proteinase enhancer stimulates procollagen processing by binding to the C-propeptide region only. *Journal of Biological Chemistry*, *286*(45), 38932–38938.

Wang, K. C., Yeh, Y. T., Nguyen, P., Limqueco, E., Lopez, J., Thorossian, S., ... Chien, S. (2016). Flow-dependent YAP/TAZ activities regulate endothelial phenotypes and atherosclerosis. *Proceedings of the National Academy of Sciences of the United States of America*, *113*(41), 11525–11530.

Wells, R. G. (2010). The role of matrix stiffness in regulating cell behavior. *Hepatology*, *47*(4), 1394–1400.

Yokoe, T., Minoguchi, K., Matsuo, H., Oda, N., Minoguchi, H., Yoshino, G., ... Adachi, M. (2003). Elevated levels of C-reactive protein and interleukin-6 in patients with obstructive sleep apnea syndrome are decreased by nasal continuous positive airway pressure. *Circulation*, *107*(8), 1129–1134.

Yong, K. W., Li, Y., Huang, G., Lu, T. J., Safwani, W. K., Pingguanmurphy, B., & Xu, F. (2015). Mechanoregulation of cardiac myofibroblast differentiation: Implications for cardiac fibrosis and therapy. *American Journal of Physiology: Heart and Circulatory Physiology*, *309*(4), H532–H542.

Yong, K. W., Li, Y., Liu, F., Gao, B., Lu, T. J., Wan Abas, W. A., ... Huang, G. (2016). Paracrine effects of adipose-derived stem cells on matrix stiffness-induced cardiac myofibroblast differentiation via angiotensin II Type 1 receptor and Smad7. *Scientific Reports*, *6*, 33067.

Yu, F. X., Zhao, B., Panupinthu, N., Jewell, J. L., Lian, L., Wang, L. H., & Guan, K. L. (2012). Regulation of the Hippo-YAP pathway by G-protein-coupled receptor signaling. *Cell*, *150*(4), 780–791.

Zhao, B., Li, L., Tumaneng, K., Wang, C. Y., & Guan, K. L. (2010). A coordinated phosphorylation by Lats and CK1 regulates YAP stability through SCF(beta-TRCP). *Genes and Development*, *24*(1), 72–85.

Zhao, H., Li, X., Zhao, S., Zeng, Y., Zhao, L., Ding, H., & Du, Y. (2014). Microengineered in vitro model of cardiac fibrosis through modulating myofibroblast mechanotransduction. *Biofabrication*, *6*(4), 045009.

Zou, Y., Akazawa, H., Qin, Y., Sano, M., Takano, H., Minamino, T., ... Komuro, I. (2004). Mechanical stress activates angiotensin II type 1 receptor without the involvement of angiotensin II. *Nature Cell Biology*, *6*(6), 499–506.

SUPPORTING INFORMATION

Additional supporting information may be found online in the Supporting Information section.